Biophysical Journal, Volume *114*

Supplemental Information

MMP Secretion Rate and Inter-invadopodia Spacing Collectively Govern Cancer Invasiveness

Sandeep Kumar, Alakesh Das, Amlan Barai, and Shamik Sen

SUPPLEMENTARY FIGURES

Characterization of thickness and stiffness of gelatin-coated substrates
For measuring gelatin thickness, coverslips were coated with fluorescent gelatin and their thickness determined using confocal microscopy. For measuring substrate stiffness, uncoated coverslips, 0.5% and 5.0% gelatin-coated glass coverslips were probed with a 4.5 μm, 67 kHz spherical AFM probe with a nominal spring constant of 60 pN/nm (Novascan). Values of spring constant and sensitivity was obtained using thermal calibration method (MFP3D). First 100 nm of indentation data was analysed using Hertz model to obtain estimates of substrate stiffness [1]. Force curves were analysed using custom written Matlab code.

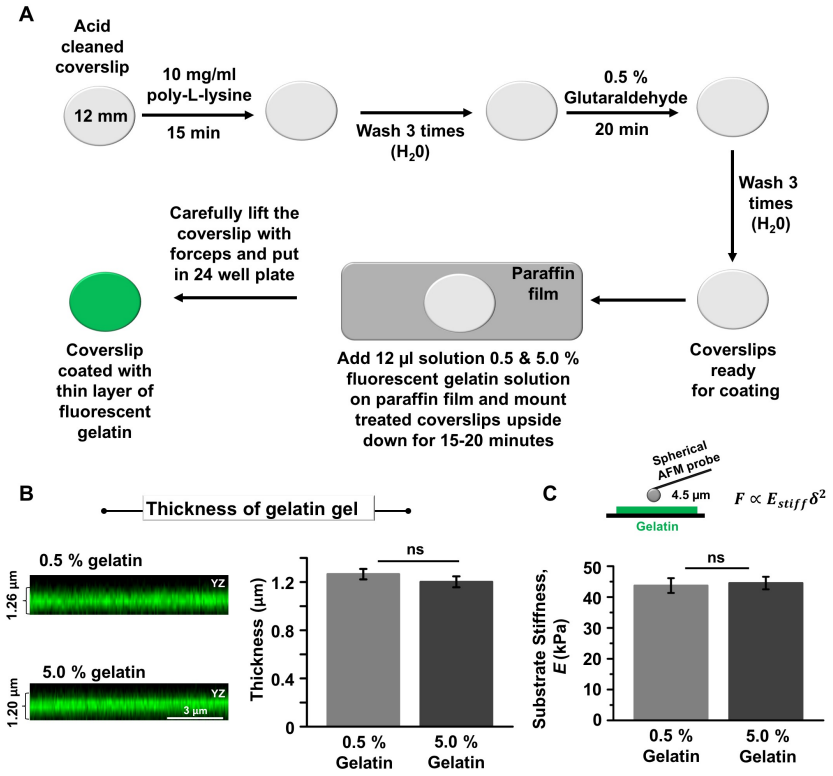

Figure S1: **Experimental procedure for gelatin coating and its characterization. (A)** Schematic for coating 12 mm coverslip with 0.5% and 5.0% fluorescent gelatin. After treating the coverslips with 10 mg/ml poly-L-lysine and then crosslinking with 0.5% glutaraldehyde, fluorescent gelatin was coated on treated coverslips by dipping them on 12 μl solution of 0.5% and 5.0% gelatin on paraffin film for 15-20 mins. **(B)** Representative confocal z-stack fluorescent images (YZ plane) of 0.5% and 5.0% gelatin coated coverslips. Thickness of gelatin layer was determined using Fiji-ImageJ software. Quantification of gelatin layer revealed no significant difference between 0.5% and 5.0% gelatin-coated substrates. Statistical significance was performed using one-way ANOVA/Fisher test (n = 2, 17-19, coverslips per condition, ns: non-significant). **(C)** Stiffness of gelatin substrates was probed with a 4.5 μm spherical probe. The first 100 nm of indentation data was fitted with Hertz model to estimate stiffness of 0.5 and 5.0% gelatin-coated substrates. Statistical significance was performed using one-way ANOVA/Fisher test (n = 2, 17-20 indentation points per sample, ns: non-significant).

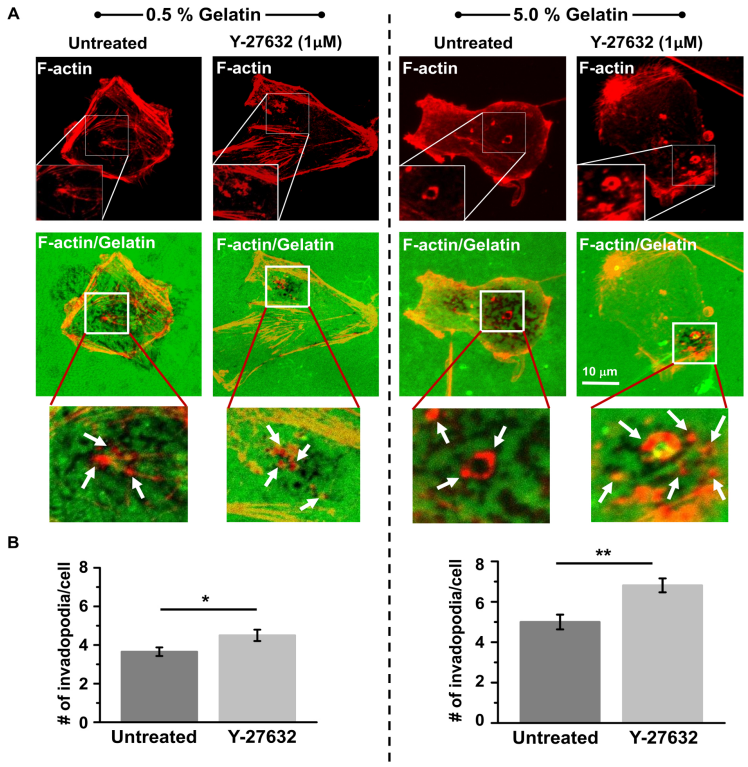

Figure S2: **Influence of Y-27632 treatment on invadopodia formation.** **(A)** Representative images of invadopodia-mediated ECM degradation in untreated and 1 μM Y-27632 treated MDA-MB-231 cells cultured on 0.5% and 5.0% gelatin-coated substrates. Scale bar = 10 μm. Co-localization of actin punta with degraded areas (white arrows) were considered as invadopodia. **(B)** Quantification of number of invadopodia/cell in untreated and Y-27632-treated cells cultured on 0.5% and 5.0% gelatin-coated substrates. Statistical significance was performed using one-way ANOVA ($n = 2$, 25-30 cells per condition; $* : p < 0.05$, $** : p < 0.01$).

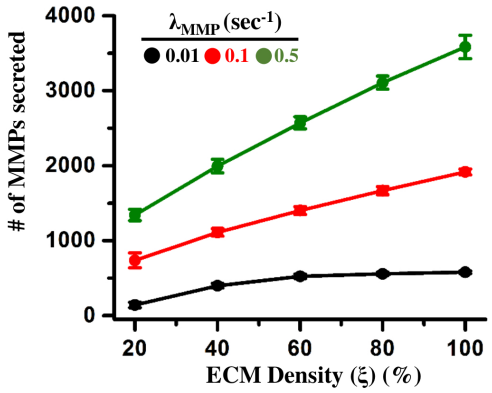

Figure S3: **MMP secretion rate and ECM density collectively regulate MMP secretion through invadopodia.** Total soluble MMP secreted by invadopodia for varying values of ECM density at three different soluble MMP secretion rate i.e., $\lambda_{MMP} = 0.01$, 0.1 and 0.5 sec^{-1}. Atleast 50 simulations per condition were performed. Error bars: $\pm$ Standard Deviation (STD).

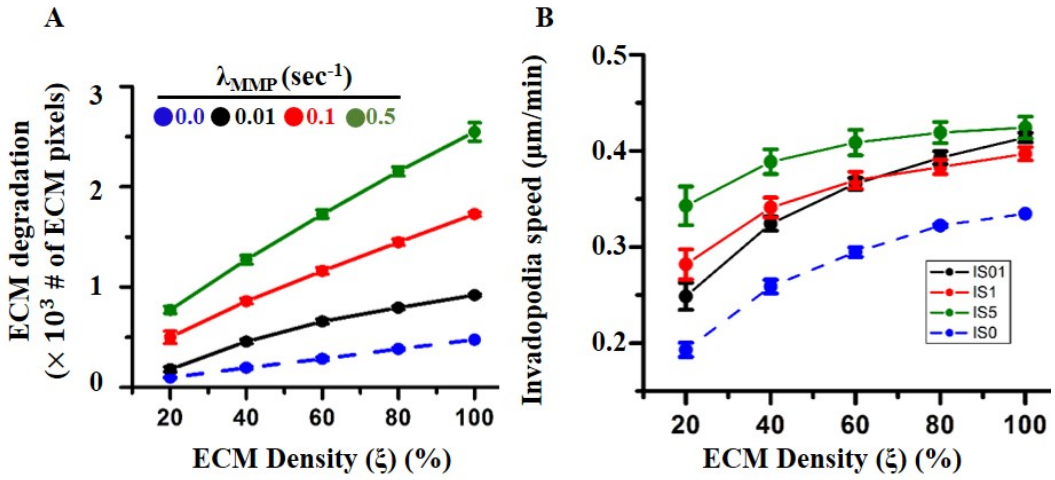

Figure S4: **Soluble MMP inhibition inhibits ECM degradation as well as invadopodia penetration. (A)** ECM degradation for varying values of ECM density at soluble MMP secretion rate i.e., $\lambda_{MMP} = 0.01$, 0.1 and 0.5 sec^{-1} and in absence of soluble MMP i.e., $\lambda_{MMP} = 0.0$. **(B)** Invadopodia speed for varying values of ECM density at soluble MMP secretion rate i.e., $\lambda_{MMP} = 0.01$, 0.1 and 0.5 sec^{-1} and in absence of soluble MMP i.e., $\lambda_{MMP} = 0.0$. Error bars: $\pm$ STD.

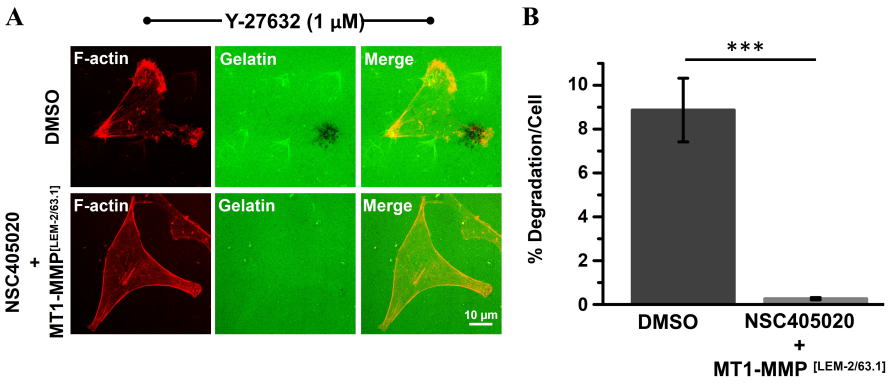

Figure S5: **MT1-MMP inhibition inhibits ECM degradation. (A)** Representative F-actin stained images of MDA-MB-231 cancer cells cultured on 5.0% fluorescent gelatin in presence of DMSO (vehicle control) and NSC405020 + MT1-MMP blocking antibody LEM-2/63.1 for 8-10 hrs. Scale bar = 10 μm. **(B)** Quantification of % degradation/cell in MDA-MB-231 cancer cells cultured on 5.0% gelatin-coated substrates in the presence of DMSO (vehicle control) and NSC405020 + MT1-MMP blocking antibody LEM-2/63.1 for 8-10 hrs. Statistical significance was performed using one-way ANOVA ($n = 2$, 25-30 cells per condition; $***: p < 0.001$). Error bar: $\pm$standard error of mean (SEM).

Invadopodia dynamics with constant aspect ratio

Increase in MMP secretion rate was observed to reduce invadopodia speed due to lack of lateral stability (Figure 4D). To probe if maintaining of aspect ration can lead to increased invadopodia activity, simulations were performed where invadopodia width was increased with increase in invadopodia height (Figure S6A). To simulate invadopodia expansion, whenever the invadopodia moved down by 2 pixels, invadopodia width was increased by 2 pixels. The ECM density and MMP concentration on these pixels were set to 0 to model instantaneous ECM degradation. The results were similar to those obtained for the previous case of fixed invadopodia width (i.e., aspect ratio changing continuously). However, for the same combination of ECM density and MMP secretion rate, ECM degradation was greater when compared to the case where aspect ratio was changing (Figures S6B, S6C).

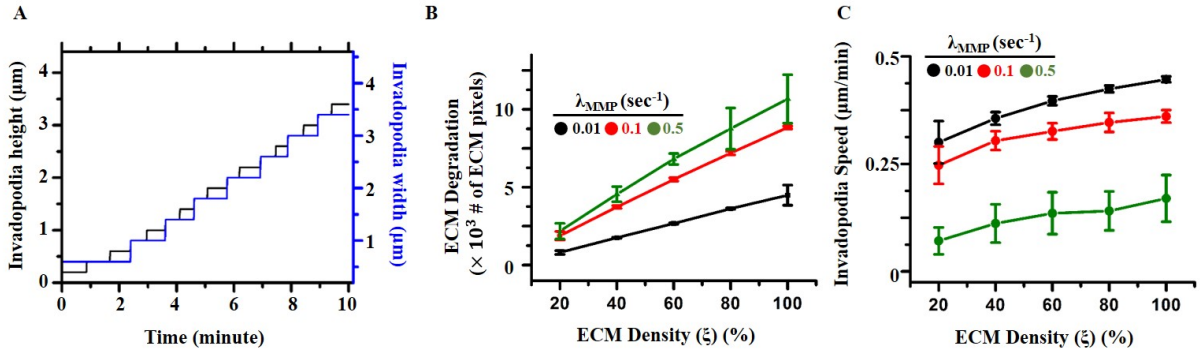

Figure S6: **Invadopodia dynamics with constant aspect ratio.** **(A)** A representative plot showing invadopodia height and width at different time points. **(B, C)** Quantification of ECM degradation and invadopodia speed for varying values of ECM density at three different soluble MMP secretion rate i.e., $\lambda_{MMP} = 0.01$, 0.1 and 0.5 sec^{-1}. Atleast 50 simulations were performed for each parameter combination to obtain the statistics. Error bars: $\pm$ STD.

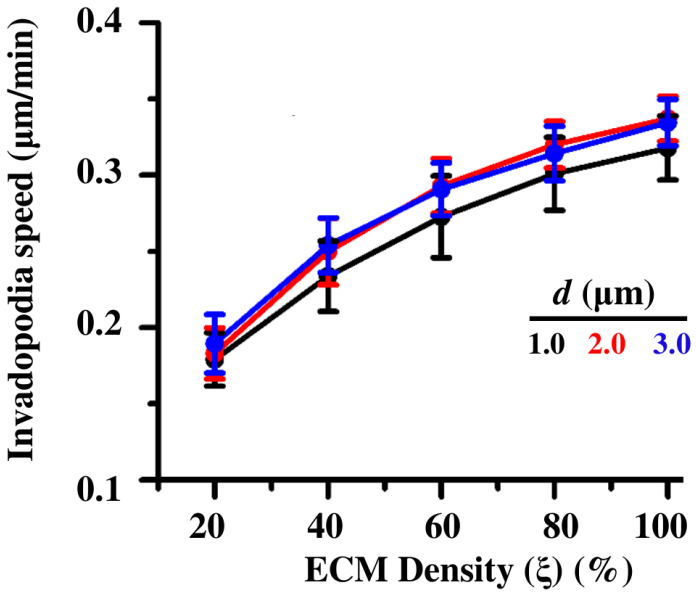

Figure S7: **Dependence of invadopodia speed on ECM density and inter-invadopodia spacing.** No major alterations in invadopodia speed was observed when inter-invadopodia spacing (d) was varied from 1 - 3 μm. Atleast 50 simulations were performed for each parameter combinations to get the statistics. Error bars: $\pm$ STD.

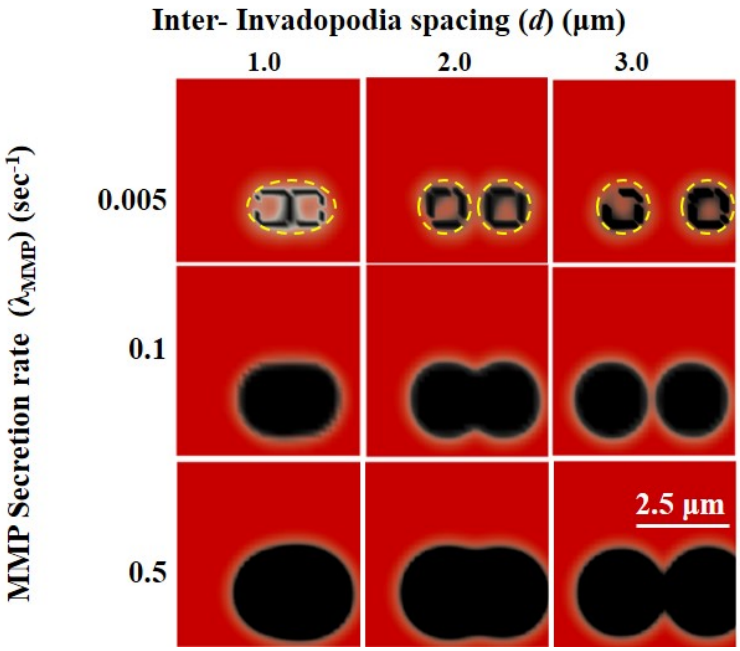

Figure S8: **Dependence of pore size on MMP secretion rate (λ_{MMP}) and inter-invadopodia spacing (d).** Representative images showing the size/shape of the degraded zones underneath the invadopodia at the end of the simulations for $d = 2$, 4 and 6 μm, and $\lambda_{MMP} = 0.005$, 0.1 and 0.5 sec^{-1}. $\xi = 100\%$. Red: ECM. Black: Degraded zone.

SUPPLEMENTARY VIDEOS

Videos V1 and V2: Videos showing single moving invadopodia (V1) and spatio-temporal ECM degradation profile (V2). $\lambda_{MMP} = 0.1$ sec^{-1}. $\xi = 100\%$.

Videos V3 and V4: Videos showing two moving invadopodia (V3) and spatio-temporal ECM degradation profile (V4). $\lambda_{MMP} = 0.1$ sec^{-1}. $\xi = 100\%$. Inter-invadopodia spacing (d) = 2 μm.

REFERENCES

[1]. J. L. MacKay and S. Kumar, Measuring the elastic properties of living cells with atomic force microscopy indentation," Cell Imaging Techniques: Methods and Protocols, pp. 313-329, 2013.